Econ. Environ. Geol.
Vol. 33, No. 1 p. 19-30, 2000.

The Sannae-Eonyang Granitic Rocks and Hydrothermal System, Southeastern Kyongsang Basin

Kyounghee Yang* and Joon Dong Lee*

ABSTRACT : The Sannae-Eonyang granitic rocks are a large fossil hydrothermal system containing the Sannae Mo-W fissure-vein type and the Eonyang amethyst deposits in the southeastern Kyongsang Basin. They evolved through similar stages showing the similarities in chemical and mineralogical compositions, fractionation trends and early magmatic fluids. Major, trace and rare earth element (REE) variations can be accounted for fractional crystallization combined with variable degrees of metasomatism. Based on the aqueous fluids exsolved directly from the crystallizing melt, the Sannae-Eonyang granitic rocks were emplaced at similar depth or pressure conditions. High temperature fluid interaction with the granitic rocks affects the elements such as K, Na, Rb, Ba, Sr, Eu, and heavy REE (HREE) mostly through feldspar re-equilibration. Although hydrothermal fluids produced partly positive Eu anomalies and HREE depletion in the granitic rocks at the Sannae Mo-W mine, the chemical concentrations defining fractionation trends have survived the effects of alteration. Aqueous fluids exsolved from the crystallizing melt appears to be widespread, whereas fluids of moderate to low salinity and low-density with relatively high homogenization temperatures and CO_2-rich fluids appear to be mainly restricted and responsible for Mo-W and amethyst mineralization, respectively. Hydrothermal system of the Sannae-Eonyang granitic rocks represents repeated fluid events; from exsolution of aqueous fluids from the crystallizing melt, through fluid immiscibility and meteoric convection to later mineralization.

INTRODUCTION

The Cretaceous granitic rocks occurring around Sannae and Eonyang area host the Sannae W-Mo deposits and the Eonyang amethyst mine in the western and eastern part of the rock suite, respectively (Fig. 1). Although there are some variations in textures and colors throughout the whole granitic rocks, abundant miarolitic cavities indicate the presence of fluids during late-stage crystallization of the magma or the nature of highly fractionated granitic rocks. The beautiful amethyst is localized in miarolitic cavities within fine-grained granitic rocks in the eastern part of the granitic rocks, whereas the Sannae W-Mo deposit is developed as a fissure-filling vein-type within medium-grained granitic rocks in the western part. Although the granitic rocks host different types of hydrothermal deposits such as amethyst and W-Mo deposits in one end and the other, they are spatially-related and probably represent separate cupolars in a relatively large pluton, suggesting different hydrothermal activities during late-stage evolution of magma or post magmatic stage.

This study has been designed to understand geochemical characteristics and the related hydrothermal systems of the Sannae-Eonyang granitic rocks. We have attempted to compare the geochemical and hydrothermal differences among granitic rocks which show productive and non-productive intrusion. Therefore, the Sannae-Eonyang granitic rocks are divided into three parts: they are the Sannae granitic rocks (SNG) hosting economic W-Mo mineralization, the barren granitic rock (MDG) and the Eonyang granitic rocks (EYG) hosting amethyst mineralization. Concentrations of major, trace, rare earth elements, and roles and characteristics of fluids which affected the granitic rocks are reported.

GEOLOGICAL SETTING

The Sannae-Eonyang granitic rocks containing the Sannae W-Mo and the Eonyang amethyst deposits are extensively exposed on the western side of the Yangsan fault line in the central part of

* Department of Geology, Pusan National University, Pusan 609-735, Korea

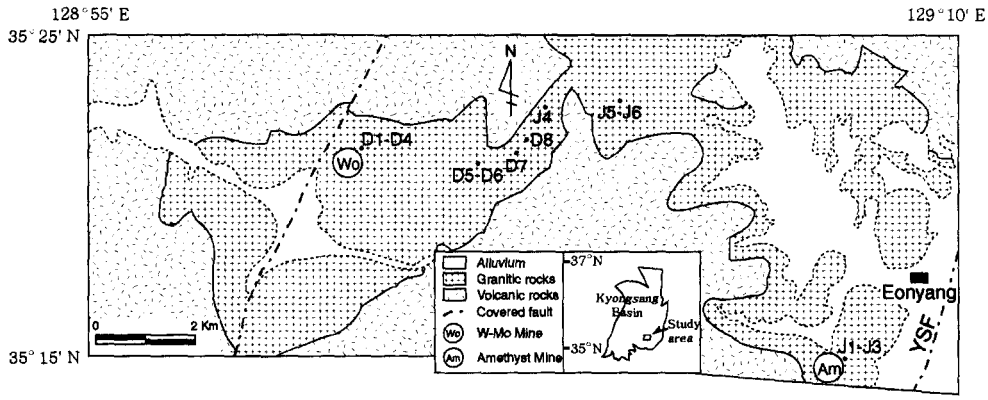

Fig. 1. Geologic map of the study area. D1-D8 and J1-J6 are sample localities. YSF=Yangsan fault.

Table 1. Modal analyses of the Sannae-Eonyang granitic rocks.

	D1	D2	D3	D5	D6	D7	D8	J1	J2	J4	J5	J6
quartz	30.6	30.4	26.3	30.3	23.8	38.3	28.5	35.8	39.4	25.7	28.4	38.9
Kfeldspar	35.4	26.3	36.9	39.7	32.6	25.7	42.3	37.1	35.4	28.6	29.4	29.9
plagioclase	25.3	25.3	23.9	22.5	32.7	27.9	22.0	24.0	23.5	40.4	39.4	28.6
biotite	2.7	10.0	5.0	2.9	6.3	4.0	3.9	1.7	1.2	2.9	2.0	1.2
hornblende	0.7	1.3	0.1	0.1	-	1.0	0.5	-	-	0.6	-	-
sericite	3.5	5.7	3.0	2.9	2.7	1.4	1.6	-	-	-	-	-
opaq. min.	0.9	0.9	0.5	1.1	1.6	1.7	1.1	1.4	0.3	0.6	0.6	1.2
chlorite	1.2	0.4	2.2	-	0.2	-	-	-	-	0.2	-	-
apatite	0.1	-	0.1	0.5	0.2	-	-	-	-	0.2	0.1	0.1
zircon	-	-	-	-	-	-	-	0.1	-	0.1	-	0.1
Total	100.7	100.3	102.0	100.3	100.1	100.0	99.9	100.1	99.8	99.9	99.9	100.0

SNG=D1-D3, MDG=D5-D8 and J4-J6, EYG=J1-J2

the Kyongsang basin (Fig. 1). They intrude Cretaceous sedimentary and volcanic rocks of the Basin. Geochronological date of the Sannae granite (SNG area) is 68 Ma by the Rb-Sr method (Kim *et al.*, 1997), whereas the Eonyang granite (EYG area) reveals as an age of 64±3 Ma by K/Ar method on biotite (Moon *et al.*, 1998), suggesting that they are probably contemporaneous. In addition, rhyolitic rocks thought to be related with the granitic rocks are 73.5±1.4 Ma by the Rb-Sr method (Hwang, 1991). The Sannae-Eonyang granitic rocks show a diversity in color and texture and contain abundant miarolitic cavities indicating fluid satura- tion during solidification. Generally, they are classified as biotite-granites. The fabric of the pluton is massive. There is no tendency for minerals to be oriented either as lineation or foliation. Schlieren composed of mafic minerals are found where subangular to ellipsoidal country rock xenoliths are common. These xenoliths and well-developed sheet joints are more common to the west of the granitic rocks.

The mineralogical compositions are almost identical through the whole pluton. The pluton is are mainly composed of quartz, K feldspar, plagioclase, and biotite. The most abundant and biggest crystals are plagioclase and K feldspar although their relative amounts and size vary in sample to sample (Table 1). Plagioclase phenocrysts often show zonal or oscillatory zoned structures. Some of plagioclase have a thin albitic rim indicating subsolidus re-equilibration. The central part of the zoned plagioclase is sometimes shattered and altered to sericite. Relatively large K feldspar is perthitic and some of them is partly altered to sericite. Quartz occurs as relict primary phenocrysts and sometimes intergrowth with alkali-feldspar in graphic textures. Porphyritic quartz are highly corroded, microfractured and broken into three or four parts showing resorbed boundaries of square shapes of an initial beta form. These highly-embayed quartz were resulted from

saline fluids in subvolcanic rocks (Donaldson and Henderson, 1988). Biotite is the dominant mafic mineral and occurs either as large crystals or as fine platy crystals disseminated in the matrix with irregular grain boundaries. Some of biotite is replaced by a combination of chlorite and sericite. Hornblende is rarely observed. Accessory minerals are zircon, apatite, sphene, magnetite, hematite and pyrite. The followings are somewhat different characteristics of granitic rocks at each area.

In the SNG area, the granites exhibit light gray-colored rock and homogeneous medium- to fine-grained equigranular texture. Compared with MDG and EYG area, the granitic rocks show more altered features. The granitic rocks containing the fissure-filling quartz veins grade into sericite-dominated rocks toward the vein margin. Alteration processes affecting the wall rock are probably related to the formation of the veins. The alteration minerals are sericite, epidote, and chlorite. Sericite occurs as fine aggregates which are irregularly distributed in the matrix or within feldspars. Quartz occurs as secondary mosaics produced during hydrothermal alteration along the vein margin. A large number of subparallel fissure-filling quartz veins are associated with Mo-W mineralization. The ore minerals of the fissure-filling quartz veins mainly include molybdenite, wolframite and scheelite (Shelton *et al.*, 1986). Milky fine-grained anhedral quartz and molybdenite were precipitated, which were followed by the deposition of prismatic, euhedral milky or clear quartz and wolframite and scheelite. Clear quartz and calcite were then deposited in the remaining open space. More detailed descriptions for the paragenesis of the minerals are referred in Shelton *et al.* (1986).

In the MDG area, the granitic rocks exhibit medium-grained seriate texture. They are as pristine as virtually any granite in which there is always a little incipient alteration.

In the EYG area, the granitic rocks exhibit coarse-grained porphyritic textures. Compared with SNG and MDG, the biggest porphyritic crystals are plagioclase although they are not as abundant as porphyritic quartz and K feldspar. Some of pinkish K feldspar are rimmed by white plagioclase showing rapakivi texture. Most amethysts are hosted in the aplite dike intruding the porphyritic biotite granite. Mialoritic cavities hosting large and high-quality amethysts are abundant in the aplite dike of the same mineral phases as the porphyritic granite. The largest cavities in the aplite dike range up to 150 cm in diameter. Euhedral quartz crystals in the cavities vary in color from white at the base of crystals to clear to purple at the terminations. The contact between aplite and the white quartz is altered to clay minerals. No alteration nor chilled margins can be found at the contact between the aplite dike and host granites.

GEOCHEMISTRY

Analytical methods

The Sannae-Eonyang granitic rocks are divided into three parts; the Sannae granitic rocks (SNG, sample D1, 2, 3, 4) hosting economic Mo-W mineralization at the Sannae mining district, the barren granitic rock at the middle area (MDG, sample D5, 6, 7, 8 and J4, 5, 6) between the Sannae and Eonyang mining district and the Eonyang granitic rocks (EYG, sample J1, 2, 3) at the Eonyang amethyst mining district. Three geochemical data at the Eonyang mining district (J1, 2, 3) and four at the middle area (J4, 5, 6, 7) are adopted from Kim (1991).

Major elements were analyzed using X-ray fluorescence (XRF) spectrometer at the Korea Basic Science Institute. The standard deviations of major elements presented by Korea Basic Science Institute are as follows:

SiO_2 0.087 TiO_2 0.001 Al_2O_3 0.016
MgO 0.014 CaO 0.002 Fe_2O_3*0.010
Na_2O 0.025 K_2O 0.009 P_2O_5 0.087
MnO 0.003

Some trace elements of granite, and REEs of granite were analyzed using Inductively Coupled Plasma mass spectrometer at the Korea Basic Science Institute. Accuracy is estimated to be within 1.5%.

RESULTS

Major and trace element concentrations are given in Table 2. Major elements vs. SiO_2 variation diagrams are shown in Fig. 2. Additional data

Table 2. Major elements, CIPW normative mineral compositions, some trace element data of the Sannae-Eonyang granitic rocks.

	D1	D2	D3	D4	D5	D6	D7	D8	J1	J2	J3	J4	J5	J6
SiO_2	74.93	74.93	76.55	76.43	74.43	72.90	72.59	73.79	76.66	76.84	76.43	72.64	73.85	73.81
TiO_2	0.19	0.21	0.09	0.19	0.21	0.29	0.31	0.26	0.19	0.14	0.18	0.29	0.22	0.20
Al_2O_3	14.05	13.97	13.32	13.46	14.17	14.55	14.91	14.27	12.42	12.73	12.65	14.23	13.89	13.95
MgO	0.24	0.26	0.04	0.15	0.35	0.87	0.52	0.40	0.25	0.11	0.17	0.40	0.30	0.24
CaO	0.89	0.93	0.88	0.46	1.26	1.41	1.63	1.20	0.66	0.44	0.45	1.12	0.84	0.75
MnO	0.07	0.07	0.05	0.14	0.07	0.08	0.08	0.08	0.09	0.06	0.10	0.09	0.08	0.06
Fe_2O_3*	1.13	1.70	0.73	0.68	1.62	2.24	2.19	1.92	1.78	1.26	1.53	2.41	2.06	1.79
Na_2O	2.85	3.36	3.05	2.12	3.52	3.61	3.66	3.36	3.56	3.82	3.63	4.18	4.00	4.17
K_2O	5.21	4.18	5.53	5.43	4.03	3.89	3.76	4.15	4.27	4.24	4.67	4.31	4.29	4.58
P_2O_5	0.04	0.02	0.00	0.05	0.05	0.08	0.08	0.05	0.04	0.02	0.03	0.07	0.05	0.05
L.O.I	0.39	2.39	0.24	0.76	0.26	0.40	0.22	0.50	0.08	0.34	0.16	0.26	0.42	0.40
Total	99.99	99.95	99.98	99.87	99.97	99.95	99.95	99.98	100.0	100.0	100.0	100.0	100.0	100.0
Normative minerals														
Qtz	36.41	37.22	43.22	44.87	35.56	33.62	32.96	35.53	37.98	37.53	36.42	29.12	32.21	30.34
Or	30.94	24.82	29.83	38.39	23.91	23.11	22.30	24.68	25.28	25.16	27.69	25.56	25.48	27.20
Ab	24.18	28.50	21.61	9.21	29.84	30.65	31.02	28.55	30.11	32.39	30.76	35.42	33.95	35.38
An	4.20	4.52	1.89	2.01	5.98	6.56	7.64	5.69	3.04	1.96	2.06	5.16	3.89	3.44
C	2.18	2.26	2.48	4.01	1.82	2.00	2.02	2.17	0.81	1.13	0.77	0.79	1.24	0.87
Hy	0.60	0.65	0.10	0.38	0.88	1.26	1.30	1.01	0.63	0.28	0.43	1.00	0.75	0.60
Mt	0.23	0.23	0.16	0.46	0.23	0.26	0.26	0.26	0.29	0.20	0.33	0.29	0.26	0.20
He	0.98	1.55	0.62	0.37	1.47	2.07	2.02	1.75	1.58	1.13	1.31	2.21	1.89	1.66
Ap	0.09	0.04	0.00	0.11	0.11	0.18	0.18	0.11	0.09	0.09	0.07	0.15	0.11	0.11
Trace elements (ppm)														
Rb	135	186	175	325	161	153	139	151						
Sr	91	150	80	57	134	181	198	134	69	43	42	128	97	97
Ba	715	945	493	993	617	675	651	690	552	182	365	653	604	707
Y	11	7	16	26	27	32	29	25	16	30	27	24	21	15
Nb	12	6	22	10	12	16	15	13	11	20	15	9	15	11
Zr	95	34	81	55	61	86	55	52	12	19	48	19	16	9
Hf	3	1	3	2	2	2	2	2						
Pb	4	16	15	11	4	15	13	11						
Th	8	5	12	13	15	10	16	14						
U	2	1	6	5	3	3	3	3						
V	7	7	3	16	9	16	16	12	13	8	9	24	21	15

*Fe_2O_3 as total Fe_2O_3. Some of trace elements for J1 to J6 are not analyzed. SNG=D1-D3, MDG=D5-D8 and J4-J6, EYG=J1-J2

of the granitic rocks from Hwang (1996), which have been collected near the Sannae mine, are also plotted in Figs. 2, 3 and 4. The Sannae-Eonyang granitic rocks are characterized by their high silica contents of a small range (72.6~76.7%), low CaO (0.44~1.63%) and high K_2O contents (3.76~5.53%) indicating that the magma was highly fractionated, and as a result, probably enriched in volatile constituents. In terms of molecular $Al_2O_3/CaO+Na_2O+K_2O$ ratios, they are metaluminous to weakly peraluminous (Fig. 3), which is comparable with those reported from the Kyongsang basin (Lee, 1991). Compared with MDG and EYG, the concentrations of Na_2O and K_2O from the SNG show somewhat a large variation probably due to alteration (Fig. 2). Except Na_2O and K_2O concentrations, all the other oxides show negative correlation with SiO_2. Na_2O is poorly correlated with silica, whereas K_2O increase with silica. Although there are some scatters, major element plots versus SiO_2 displays a fractionation trend.

Trace elements vs. SiO_2 variation diagrams are shown in Fig. 4. A fractionation is indicated by the increase in Rb and decrease in Sr and V with increase of SiO_2, whereas Ba show positive correlation with SiO_2 until 76 wt% and then decrease

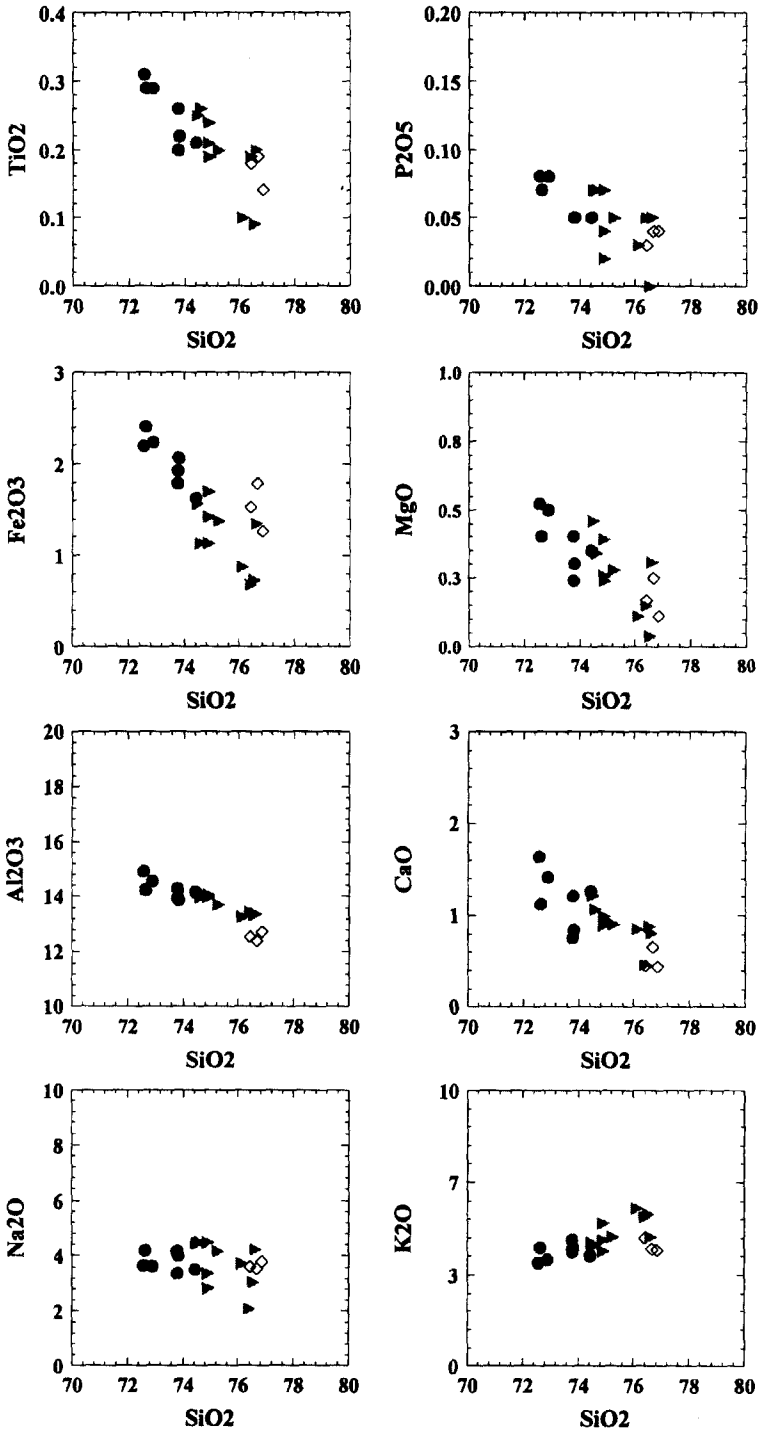

Fig. 2. Major elements vs. SiO_2 variation diagrams of the Sannae-Eonyang granitic rocks. Symbols: filled circle= MDG, filled triangle=SNG, Diamond=EYG.

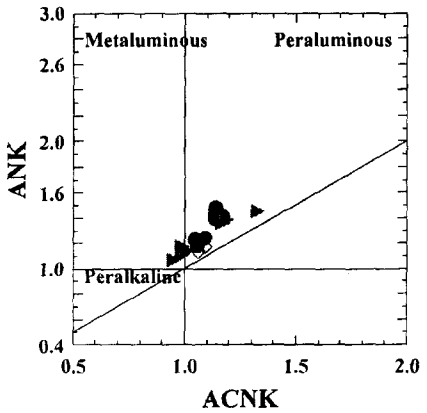

Fig. 3. Molar $Al_2O_3/(Na_2O+K_2O)$ vs. $Al_2O_3/(CaO+Na_2O+K_2O)$ diagram of the Sannae-Eonyang granitic rocks. Symbols as for Fig. 2.

(Fig. 4). Variation trends in Ba and Sr probably reflect K-feldspar fractionation during crystallization of the granites, whereas scattered data may be resulted from alteration (Fig. 5). Petrographically, K-feldspars are more abundant than plagioclases in most samples, suggesting K-feldspar played a dominant role for the controlling the fractionation trend of the melt. However, concentrations of some trace elements such as Y, Zr, Nb, and Th are highly variable and thus variation trends are not well defined.

REE concentrations are given in Table 3. Chondrite-normalized REE patterns are shown in Fig. 6. Because of its extremely low REE contents, sample D1 is not plotted and not further discussed. The data of MDG and EYG from Kim (1991) also are plotted. The REEs, in general, decreased in amounts with increasing atomic number in LREE, whereas HREE show flat and complicated features, indicating that fractionation of garnet or/ and zircon were not significant. Eu anomaly ranges from negative to either markedly less negative or positive. The REE patterns of the SNG (Fig. 6a) is characterized by the depletion of HREE ($(Ce/Yb)_{CN}$=1.67-26.78) and one positive (Eu/Eu*=1.32) and two negative Eu anomalies (Eu/Eu*=0.49-0.57). The MDG (Fig. 6b) is depleted in HREE ($(Ce/Yb)_{CN}$=2.36-8.63) and show little Eu anomaly (Eu/Eu*=0.62-1.06). The EYG show the similar variation to those from SNG and MDG except for the larger negative Eu anomalies (Fig. 6c). Moon *et al.*, (1998) also reported REE patterns of the EYG showing similar negative Eu anomaly and flat HREE-depleted.

The Eu anomaly is related to the amount of plagioclase in magma. REE patterns of the EYG shows more enhanced plagioclase fractionation than SNG and MDG since increasingly larger negative Eu anomalies indicate the progressive removal of plagioclase from the magma. Petrographic observations show that the earliest crystallizing phases were quartz, K feldspar, and plagioclase leading to the formation of porphyritic rocks in the EYG containing large crystals of these minerals before pressure quenching, whereas the SNG and MDG show medium- to finegrained equigranular or seriate. These data are consistent with more enhanced plagioclase or K feldspar fractionation and thus, more negative Eu anomaly.

HYDROTHERMAL FLUIDS

Fig. 7 show major hydrothermal fluids trapped in SNG, MDG and EYG, respectively, which are summarized in Table 4. These pictures are arranged in temporal sequences showing different evolving fluid histories during the late- or post-magmatic stage for each examined granitic rocks (Yang, 1996; Yang and Lee, 1998). The early fluids trapped in magmatic quartz are strikingly identical in phase ratios, salinities, and homogenization temperatures in the SNG, MDG, and EYG (Table 4). Afterwards, fluids underwent different hydrothermal evolution probably due to the local tectonic characteristics or variations in the water-rock mass ratio within the granitic rocks.

In the SNG area (Fig. 7; S1-S3), the second fluids (Fig. 7S2 and S3) responsible for the Mo-W mineralization are observed in the subparallel fissure-filling quartz veins cementing the host granitic rocks. It seems these fluids were generated by fluid-host rock interactions because of its wide salinity range within the same generation and narrow homogenization temperature ranges (Table 4). In addition, these fluids are only observed with the quartz veins in the SNG area. Metals may be selectively leached from wall rocks by hot circulating fluids. The quartz veins became a conduit for deep-seated fluids during uplift and dilatancy. As described in the previous section, alteration processes affecting the wall rock along

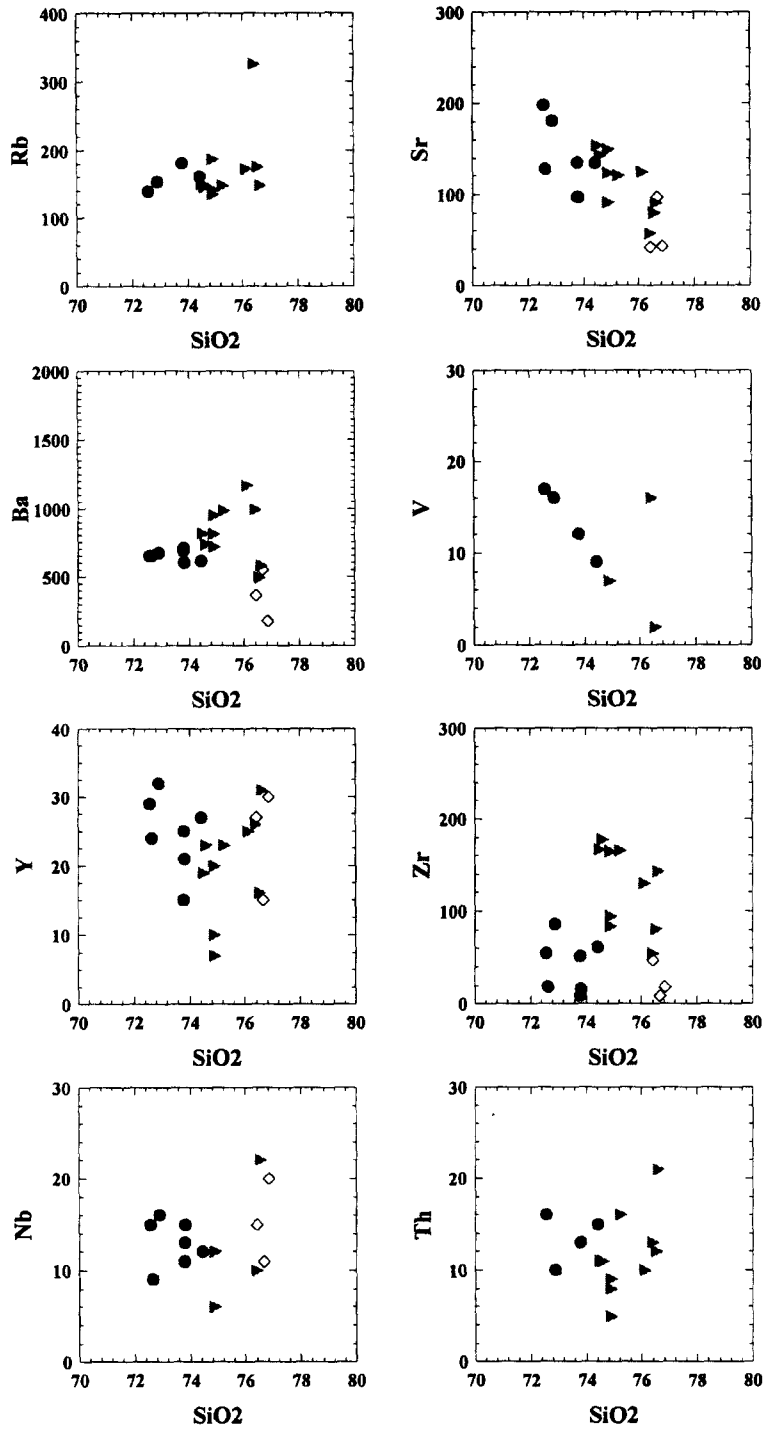

Fig. 4. Trace elements vs. SiO_2 variation diagrams of the Sannae-Eonyang granitic rocks. Symbols as for Fig. 2.

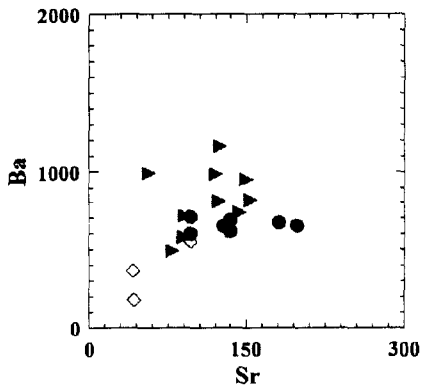

Fig. 5. Ba vs Sr diagram of the Sannae-Eonyang granitic rocks. Symbols as for Fig. 2.

the vein margins were probably related to these fluids. The fluids were mixed with circulating meteoric fluids and then cooled and diluted to form hydrothermal fluids of lower temperature and lower salinity to be trapped as inclusions during the final stage of hydrothermal activity.

The characteristic feature of fluids in the MDG area (Fig. 7; M1-M3) is the boiling responsible for the precipitation of quartz in the miarolitic cavities (Fig. 7M2, Table 4). Fluid boiling continued from the beginning of quartz crystallization in miarolitic cavities to its completion (Fig. 7M3). This boiling fluids can indicate the P-T conditions of the mineralization in the cavities (Yang and Lee, 1999). Compared with pressure estimations in the SNG and EYG (Yang, 1996; Yang and Lee, 1999), it was relatively a low pressure system. This low pressure system of the MDG area may be predominately induced by hydrostatic rather than

Table 3. Rare earth element data of the Sannae-Eonyang granitic rocks.

	D1	D2	D3	D4	D5	D6	D7	D8	J1	J2	J3	J4	J5	J6
La	3.86	31.1	24.4	47.0	37.7	13.1	24.9	19.0	9	11	17	38	22	36
Ce	10.08	61.0	45.1	98.1	77.6	26.7	54.1	4.1	714	20	30	69	35	65
Pr	0.99	6.71	6.44	12.1	8.67	3.24	6.36	5.09						
Nd	3.68	21.3	21.2	42.1	28.2	12.4	23.0	18.1	5	7	11	25	15	22
Sm	0.85	2.98	3.88	8.65	4.92	3.04	4.60	3.87	1.4	2.5	2.8	4.7	3.3	4.4
Eu	0.57	1.18	0.68	1.26	0.96	1.13	1.11	1.00	0.4	0.2	0.3	0.7	0.6	0.6
Gd	1.05	2.36	3.24	6.47	4.28	3.49	4.26	3.51						
Tb	2.01	0.31	0.51	0.92	0.69	0.60	0.69	0.59						
Dy	1.47	1.53	3.04	4.66	3.91	4.01	4.18	3.63	1.6	3.4	3.0	2.8	2.6	2.6
Ho	0.35	0.21	0.52	0.69	0.72	0.84	0.78	0.68						
Er	1.20	0.65	1.63	2.13	2.16	2.67	2.45	2.07						
Tm	0.22	0.08	0.27	0.30	0.33	0.40	0.37	0.32						
Yb	1.56	0.59	2.00	2.22	2.33	2.93	2.54	2.29	1.5	3.3	3.1	2.2	2.1	1.3
Lu	0.22	0.09	0.31	0.33	0.37	0.42	0.38	0.36						
ΣREE	28.11	130.09	113.22	226.93	172.84	74.97	129.82	102.21						
$(Ce/Yb)_{CN}$	1.67	26.78	5.85	11.39	8.63	2.35	5.52	4.72						
$(Eu/Eu^*)_{CN}$	1.84	1.32	0.57	0.49	0.62	1.06	0.75	0.81						

Some of elements in J1 to J6 are not analyzed. SNG=D1-D3, MDG=D5-D8 and J4-J6, EYG=J1-J2

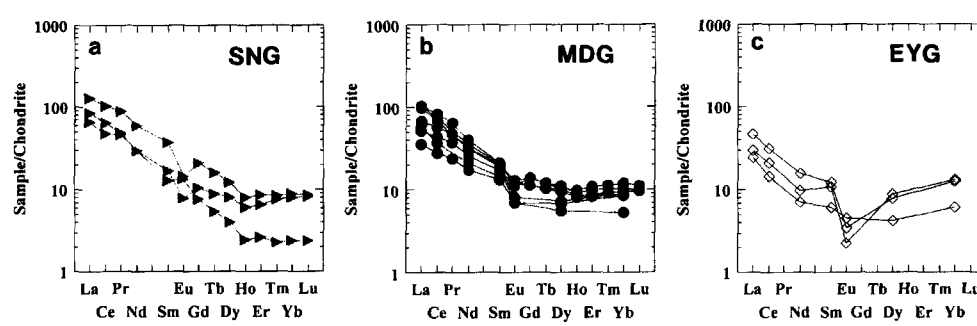

Fig. 6. Chrondrite-normalized REE patterns of the Sannae-Eonyang granitic rocks. (a) Sannae mining district (SNG), (b) middle area (MDG), (c) Eonyang amethyst mining district (EYG) of the Sannae-Eonyang granitic rocks.

Table 4. Fluid inclusion data of the Sannae-Eonyang granitic rocks. Salinity and Homogenization temperatures (Th) are adopted from Yang and Lee (1999)*, and Yang (1996)**

Area	Type of inclusion	Salinity (equiv.wt%NaCl)	Th (°C)
*Sannae W-Mo deposits (SNG) (Fig. 7; S1-S3)	1. halite-bearing (Fig. 6a)	37-41	305-337
	2. aqueous, liquid-rich (Fig. 6b)	3-24	309-473
	3. aqueous, liquid-rich (Fig. 6c)	5-14	425-429
*Middle barren area (MDG) (Fig. 7; M1-M3)	1. halite-bearing (Fig. 7a)	38-43	306-359
	2. halite-bearing and vapor-rich (Fig. 7b)	34-38	303-390
		0-7	370-465
	3. halite-bearing and vapor-rich (Fig. 7c)	36-37	333-376
		0-1	380-390
**Eonyang amethyst deposits (EYG) (Fig. 7; E1-6E3)	1. halite-bearing (Fig. 8a)	30-38	320-380
	2. halite-bearing (Fig. 8b)	33-34	320-333
	3. CO_2-bearing (Fig. 8c)	8-9	273-288

lithostatic conditions. Alternatively, the mineralization in the miarolitic cavities in the MDG area was either the late event that much uplifting and erosion of the host rocks took place.

In the EYG area (Fig. 7; E1-E3), the second fluids (Fig. 7E2) responsible for precipitating quartz or amethystine quartz in the miarolitic cavities are of high-salinity and has been interpretated as magmatic fluids (Yang, 1996; Moon *et al.*, 1998). Moon *et al.* (1998) reported that all quartz in the miarolitic cavities were formed from magmatic fluids based on the isotope data. The third CO_2-rich fluids (Fig. 7E3) were probably the major fluids for precipitating amethyst since they are mainly observed in the amethystine quartz (Yang, 1996). It was a final characteristic fluid event which appears to be locally restricted to the eastern part of the Sannae-Eonyang granitic rocks.

DISCUSSIONS

According to experimental evidence and numerical modeling (Shinohara *et al.*, 1989; Cline and Bodnar, 1991), partitioning of chlorine between coexisting aqueous fluids and melt is a function of the pressure in the system. Large amount of chlorine exsolve from a typical calc-alkaline melt at higher pressure. In addition, phase equilibrium constraints homogenized by halite dissolution at temperatures above Th(L-V) suggest that fluids were exsolved directly from the crystallizing magma and trapped at high pressure systems (Cline and Bodnar, 1991, 1994, Bodnar and Vityk, 1994, Yang and Lee, 1998). In the Sannae-Eonyang granitic rocks, the earliest fluids are strikingly identical in phase ratios, salinities, and homogenization temperatures and phase equilibrium constraints that homogenized by halite disappearance at temperatures above the vapor bubble disappearance during microthermometry in three examined areas, SNG, MDG and EYG (Fig. 7; S1, M1, and E1; Table 4). These informations suggest they were trapped in magmatic quartz at the similar depth or at the similar solidus pressure-temperature condition.

There is disagreement about the behavior of trace elements during hydrothermal alteration. Bajwah *et al.* (1995) suggested that the variation in trace element concentrations of altered granites are related to fractionation. They even showed that highly altered rocks still had primary geochemical concentrations. On the other hand trace element variations in the granitic rocks are thought to be the result of hydrothermal alteration (Higgins *et al.*, 1985). In the case of the Sannae-Eonyang granitic rocks, the chemical concentrations defining fractionation trends of igneous origin have survived the effects of alteration. The extent of scattered-variations may depend on the extent of alteration of the primary feature.

Michard (1989) demonstrated that fluids with high temperature (>230), high chlorine content and low pH (<6) showed a positive Eu anomaly, regardless of the rock type. The positive Eu anomalies of SNG resulted probably from the metasomatic reaction due to high temperature fluid interaction, that is, by high-salinity solutions which already had developed Eu anomalies owing to the

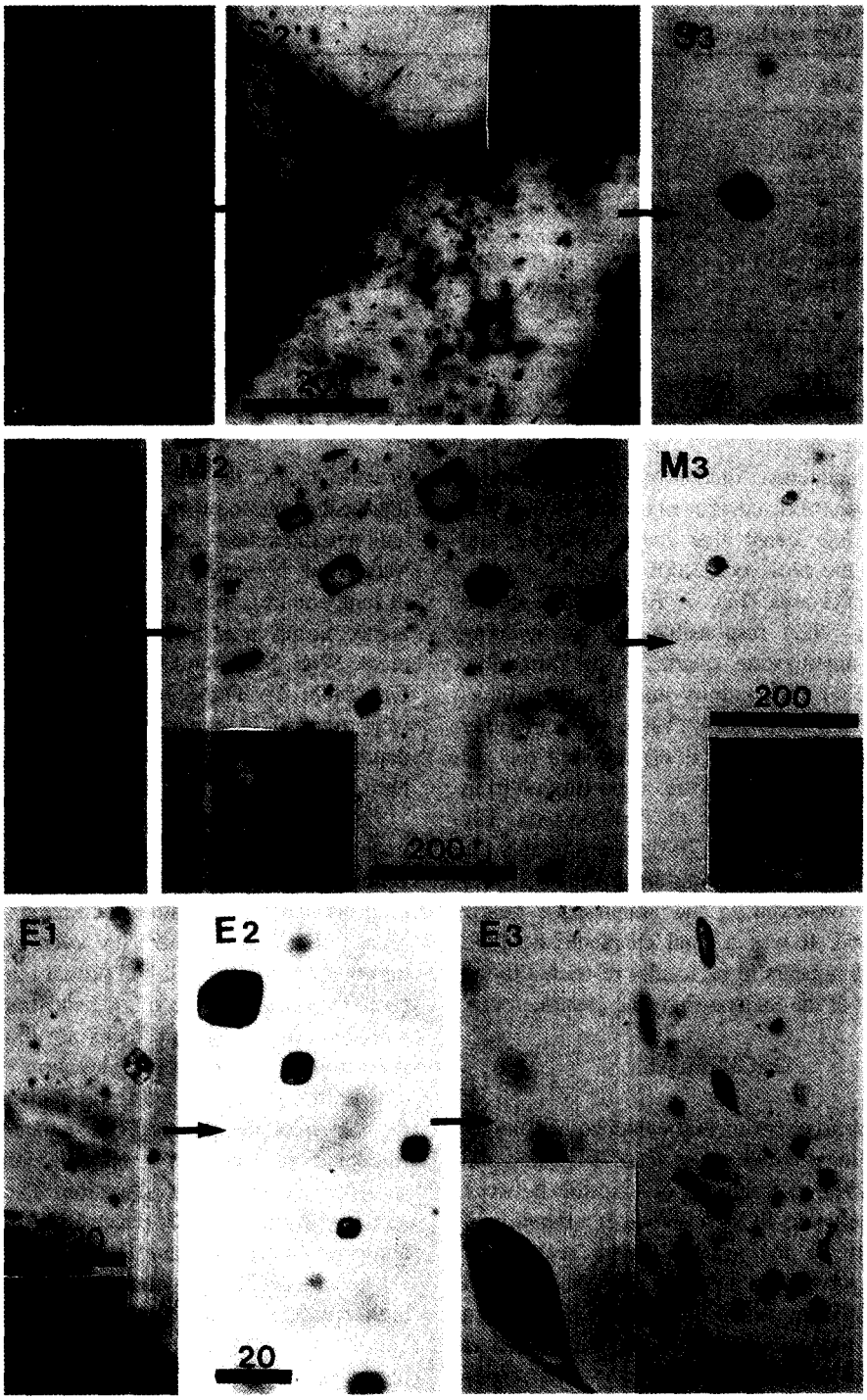

Fig. 7. Photomicrographs showing textures of primary fluid inclusions trapped in the Sannae Mo-W mine (SNG, S1-S3), middle area (MDG, M1-M3), and Eonyang amethyst mine (EYG, E1-E3) of the Sannae-Eonyang granitic rocks. The arrows indicate the temporal sequences at each granitic rocks. The numbers on the scale bars are in micron (μm).

alteration of feldspar. Another possibility for the positive Eu anomalies in feldspar-rich granitic rocks may be the incomplete separation of feldspar and liquid due to the viscosity of the magma (Henderson, 1984). The granitic rocks from the Kyongsang basin have been reported to show the negative Eu anomalies (Kim and Kim, 1997; Lee, 1997). MDG is a petrographically fresh granitic rocks as a common granitic rock observed in the Kyongsang basin. We assumed that the positive Eu anomaly in the MDG resulted from the analysis of an anomalous sample containing more concentrated feldspar. However, the positive anomaly is not so significantly high (Eu/Eu*=1.06) to be seriously discussed.

Although the rare earth elements (REEs) are regarded as the least soluble trace elements and are relatively immobile during weathering and hydrothermal alteration (Rollinson, 1993), the REEs become very soluble in CO_2-rich or saline fluids. The hydrothermal fluid play a major role in the removal and transportation of the REEs during hydrothermal alteration (Henderson, 1984; Michard, 1989). Moreover, the depletion of HREEs are due to saline brines where HREE are transported more readily in saline brines and CO_2-rich fluids (Mysen, 1979; Michard, 1989; Rollinson, 1993). HREEs of the Sannae-Eonyang granitic rocks show highly variable compositional trends compared with LREEs (Fig. 5), which are probably produced by the metasomatic reaction due to high temperature fluid interaction of high-salinity solutions. The interaction between the granitic rocks and high temperature fluid affects elements such as K, Na, Rb, Ba, Sr, Eu, and HREE mostly through feldspar re-equilibration. Based on the petrographic and geochemical criteria, the SNG experienced more enhanced hydrothermal alteration along the contacts with the quartz veins as input conduits of new high temperature fluids.

CONCLUSIONS

The Sannae-Eonyang granitic rocks show a diversity in color, texture, and mineralogy. These textural varieties probably resulted from local variations in the crystallization history of a single magma body, which can be inferred from their chemical and mineralogical similarities, fractionation trends, and magmatic fluids patterns with even some scatters. The textural variation can be explained by a pressure quenching of partially crystallized magma near the roof of the body, which is common in a near-surface intrusion (Bajwah, 1995). Based on the data from the aqueous fluid inclusions exsolved directly from the crystallizing melt, the Sannae-Eonyang granitic rocks is suggested to have been emplaced at similar depth or similar solidus pressure-temperature conditions. However, three examined granitic rocks contain different late- or postmagmatic fluids indicating that these fluids played different roles for characteristic mineralizations such as Mo-W, or amethyst precipitation. Hydrothermal activity of the Sannae-Eonyang granitic rocks was represented by exsolution of widespread aqueous fluids from the crystallizing melt and fluids of moderate to low saline and low-density and CO_2-rich fluids apparently restricted to the Sannae and Eonyang mines, respectively. The Sannae-Eonyang granitic rocks show a locus for repeated fluid events due to thermal, tectonic and acidic compositional properties of the magma, which encouraged molybedenite and tungsten and amethyst mineralization.

ACKNOWLEDGMENTS

We would like to thank Professor K.W. Min, M.E. Park, and an anonymous reviewer for improving many points in the text. The present study was supported by the settlement research fund of Pusan National University for a newly-appointed Professor and the Matching Fund Programs of Research Institute for Basic Sciences (project No. RIBS-PNU-98-501).

REFERENCES

Bajwah, Z.U., White, A.J.R., Kwak, T.A.P, and Price, R.C. (1995) The Renison granite, Northwestern Tasmania: A petrological, geochemical and fluid inclusion study of hydrothermal alteration. Econo. Geol., v. 90, p.1663-1675.

Bodnar, R.J. and Vityk, M.O. (1994) Interpretation of microthermometric data for H_2O-NaCl fluid inclusions: In: Vivo, B. De and Frezzotti, M.L. (eds.), Fluid Inclusions in Minerals, Methods and Applications. Virginia Polytechnic Institute and State University, VA, p. 117-130.

Cline, J.S. and Bodnar, R.J. (1991) Can economic porphyry copper mineralization be generated by a typical calc-alkaline melt? Jour. Geophy. Research, v. 96, p. 8113-8126.

Cline, J.S. and Bodnar, R.J. (1994) Direct evolution of brine from a crystallizing silicic melt at the Questa, New Mexico, Molybdenum deposit. Economic Geolology, 89, 1780-1802.

Donaldson, C.H. and Henderson, C.M.B. (1988) A new interpretation of round embayments in quartz crystals. Mineral. Magazine, v. 52, p. 27-33.

Henderson, P. (1984) Rare earth element geochemistry. Elsevier, New York, 510p.

Higgins, N.C., Solomon, M. and Varne, R. (1985) The genesis of the Blue Tier Batholith, northeastern Tasmania, Australia. Lithos, v. 18, p. 129-149.

Hwang, S.G. (1996) On the geology and fluid inclusion study in Sannae tungsten deposit and its vicinity. Unpub. M. S. thesis, Pusan Nat. Univ., 86pp.

Hwang, S.K. (1991) Volcanology and petrology of the Cretaceous volcanic rocks in the Central Yuncheon subbasin. Korea. Ph. D. thesis, Kyungpook Nat. Univ. 199p. (*in Korean with English abstract*)

Kim J.Y. (1991) A Petrological study on the Eonyang granite in Eonyang, Gyeongsang-Namdo. Unpub. M. S. thesis, Pusan Nat. Univ., 38pp.

Kim, C. and Kim, G. (1997) Petrogenesis of the early Tertiary A-type Namsan alkali granite in the Kyongsang Basin, Korea. Geoscience Journal, v. 1, p. 99-107.

Kim, G., Kim, J. and Park, M (1997) Rb-Sr age-dating on the granitic rocks in the Kyongsang basin. Jour. Petro. Soc. Korea, abstracts, v. 6, p. 20.

Lee, J.I. (1991) Petology, mineralogy and isotopic study of the shallow-depth emplaced granitic rocks, Southern part of the Gyeongsang Basin, Korea, -Origin of micrographic granite-. Unpub. Ph. D. Dissertation, University of Tokyo.

Lee, J.I. (1997) Trace and rare earth element geochemistry of granitic rocks, southern part of the Kyongsang basin, Korea. Geoscience Journal, v. 1, p. 167-178.

Michard, A. (1989) Rare earth element systematics in hydrothermal fluids. Geochim. et Cosmo. Acta, v. 53, p. 745-750.

Moon, S.H., Park, H., Ripley, E.M., and Hur, S.D. (1998) Petrography and stable isotopes of granites around the Eonyang rock crystal deposits. Jour. Geol. Soc. Korea, v. 34, p. 211-227.

Mysen, B.O. (1979) Trace element partitioning between garnet peridotite minerals and water-rich vapor. Ameri. Mineral., v. 64, p. 274-287.

Rollinson, H. (1993) Using geochemical data: evaluation, presentation, interpretation. Longman scientific & technical, New York, 352p.

Shelton, K.L., So, C.S., Rye, D.M., & Park, M.E. (1986) Geologic, sulfur isotope, and fluid inclusion studies of the Sannae W-Mo mine, Republic of Korea: Comparision of sulfur isotope systematics in Korean W deposits. Econo. Geol., v. 81, p. 430-446.

Shinohara, H., Iiyama, J.T. and Matsuo, S. (1989) Partition of chlorine compounds between silicate melt and hydrothermal solutions: I. Partition of NaCl-KCl. Geochim. et Cosmo. Acta, v. 53, p. 2617-2630.

Yang, K. (1996) The use of fluid inclusions to constrain P-T-X conditions of formation of Eonyang amethyst. Jour. Petro. Soc. Korea, v. 5, p. 1-9.

Yang, K. and Lee, J.Y. (1998) Fluid inclusion of the Ilkwang Cu-W-bearing breccia-pipe deposit, Kyongsang Basin. Geoscience Journal, v. 2, p. 15-25.

Yang, K. and Lee, J.D. (1999) A fluid Inclusion of the Sannae granite and the Sannae W-Mo deposit, Southeasten Kyongsang Basin. Jour. Petro. Soc. Korea, v. 8, p. 47-56.

1999년 6월 30일 원고접수, 2000년 2월 9일 게재승인.

경상분지 남동부의 산내-언양 화강암류와 열수계

양경희* · 이준동*

요 약 : 경상남도 남동부에 위치하고 있는 산내-언양 화강암류는 산내지역에 몰리브데니움와 텅스텐광상, 언양지역에 자수정광상을 배태하고 있는 화석열수계를 나타내고 있다. 이 화강암류는 국부적으로 조직의 변화를 보여주고 있으나, 화학 및 광물조성, 분별경향, 마그마에서 용리된 초기열수가 매우 유사하여, 하나의 마그마체가 결정화되어진 것으로 여겨진다. 주원소, 미량원소, 희토류원소의 변이는 분별결정작용과 열수용액의 교대작용에 의한 것으로 설명되어진다. 결정화되고 있는 마그마에서 용리된 열수유체에 의하면, 산내-언양 화강암류는 거의 유사한 깊이(압력)에 정치한 것으로 여겨진다. 화강암체와 고온의 열수와의 상호작용에 의하여 화강암체의 K, Na, Rb, Ba, Sr, Eu와 HREE 성분에 영향을 주었으며, 대부분 장석의 재평형에 의한 것으로 보인다. 산내광상지역에서는 열수에 의해 부분적으로 정 Eu 이상과 HREE 결핍을 초래했으나, 분별경향을 나타내는 화학조성은 보존되어있다. 마그마의 결정후기에 용리되어진 열수는 화강암체 전역에서 관찰되나, 높은 균질화 온도를 가지면서 저-중염도의 유체와 CO_2가 풍부한 열수는 이 화강암체의 몰리브데니움-텅스텐광상과 자수정광상이 있는 서쪽과 동쪽에서 각각 제한되어 나타난다. 산내-언양 화강암류의 열수계는 마그마에서의 열수의 용리, 열수의 비등, 기상수와의 혼합, 열수광화대로 표현되어지고 있다. 주요어: 산내-언양, 화강암류, 열수계, 분별결정작용, 교대작용, 용리